Structural Chemistry
https://doi.org/10.1007/s11224-019-01371-4

ORIGINAL RESEARCH

Water-induced isomerism of salicylaldehyde and 2-acetylpyridine mono- and bis-(thiocarbohydrazones) improves the antioxidant activity: spectroscopic and DFT study

Mohamed H. Assaleh[1] · Aleksandra R. Božić[1] · Snežana Bjelogrlić[2] · Milena Milošević[3] · Milena Simić[4] · Aleksandar D. Marinković[1] · Ilija N. Cvijetić[5]

Received: 20 March 2019 / Accepted: 3 June 2019

Abstract

Thiocarbohydrazones (TCHs) and structurally related molecules are versatile organic compounds which exert antioxidant, anticancer, and other beneficial health effects. The combination of UV/Vis, NMR spectroscopy, and quantum chemical calculations was used to rationalize the experimentally observed increase in the radical scavenging activity upon the addition of water in DMSO solution of TCHs. Mono- and bis(salicylaldehyde) TCHs (compounds **1** and **2**) undergo water-induced *E*-to-*Z* isomerization which is followed by disruption of intramolecular hydrogen bond, ground state destabilization, and 11 kcal/mol decrease in the bond dissociation enthalpy (BDE). Electron spin delocalization is more pronounced in *Z*-isomers of **1** and **2**. On the other hand, 2-acetylpyridine TCHs (compounds **3** and **4**) undergo thione-to-thiol tautomerism which also decreases the BDE and facilitates the hydrogen atom transfer to 2,2-diphenyl-1-picrylhydrazyl radical (DPPH$^{\cdot}$). The appearance of thiolic –SH group as another reactive site toward free radicals improves the antioxidant activity of **3** and **4**. The spin density of **3**- and **4**-thiol radicals is delocalized over the entire thiocarbohydrazide moiety compared to more localized spin of thione radicals. Additional stabilization of thiol radicals corroborates with the increased antioxidant activity. This study provides the new insights on the solution structure of TCHs, and also highlights the importance of solution structure determination when studying the structure-antioxidant relationships of isomerizable compounds.

Keywords Thiocarbohydrazones · *E*/*Z* isomerism · Tautomerism · Antioxidant activity · Bond dissociation enthalpy · Spin density distribution

Electronic supplementary material The online version of this article (https://doi.org/10.1007/s11224-019-01371-4) contains supplementary material, which is available to authorized users.

✉ Ilija N. Cvijetić
ilija@chem.bg.ac.rs; ilija042@yahoo.com

[1] Faculty of Technology and Metallurgy, University of Belgrade, Karnegijeva 4, Belgrade, Serbia

[2] National Cancer Research Center of Serbia, Pasterova 4, Belgrade, Serbia

[3] SI Institute of Chemistry, Technology and Metallurgy, National Institute, Department of Ecology and Techoeconomic, University of Belgrade, Njegoševa 12, Belgrade, Serbia

[4] Faculty of Pharmacy, University of Belgrade, Vojvode Stepe 450, Belgrade 11000, Serbia

[5] Innovation Center of the Faculty of Chemistry, University of Belgrade, Studentski trg 12-16, Belgrade, Serbia

Introduction

Thiocarbohydrazide is a promising unit to synthesize new polyfunctional thiocarbohydrazones (TCHs) after condensation with an aldehyde or ketone [1]. Biological activities of TCHs are the functions of their parent aldehyde or ketone moiety, and therefore it is very important to foresee the optimal structural fragments giving the improved biological activity [2]. Also, TCHs contain an azomethine (–C=N–) linkage that may connect two or more aromatic/heterocyclic ring to form various molecular hybrids with interesting biological properties [3]. In addition, TCHs and structurally similar thiosemicarbazones are well-studied anticancer agents [4–7], but also exert other biological activities [2, 8, 9].

TCHs are structurally versatile molecules with several possible solution structures including configurational (*E* or *Z*) isomers around imine bond and thione/thiol tautomers

Published online: 19 June 2019

[10–12]. The state of equilibria depends on energy of appropriate form, solvent/solute interactions and intra/intermolecular hydrogen bonding [13]. Hydrogen bonding interactions determine the geometry and interaction/functionality of biologically active compounds. Therefore, knowledge of the mechanism of hydrogen bond formation and subsequent influences on molecular properties is very important for the design of molecules with the improved biological profile. A photochromism of 2-hydroxyphenyl and 2-pyridyl(carbohydrazones) results in *E/Z* isomerization driven by the intramolecular hydrogen bond in *E*-2-hydroxyphenyl and *Z*-2-pyridyl derivatives [14]. The bis(hydrazones) with 2-pyridyl moiety represent an interesting class of tunable molecular switches where the isomerism from stable *E*,*E* isomer to metastable *E*,*Z* and *Z*,*Z* forms can be controlled photochemically or electrochemically [15].

2-Acetylpyridine and 2-hydroxybenzaldehyde are aromatic carbonyl compounds and constitute the compounds with promising biological activities [16, 17], probably due to their chelating ability toward vital metal ions [18, 19]. TCHs are able to interact with many metalloenzymes essential for microbes [12], while sulfur atom increases lipophilicity which is generally positively correlated with potency [20]. The Schiff bases are also known for their antioxidant activities. Two aromatic rings of diarylhydrazones linked with (carbo)hydrazide moiety represent an interesting pharmacophore for antioxidant activity [21]. The extended conjugation is the characteristics of natural antioxidants such as lycopene and β-carotene, and can be achieved through the rapid equilibrium between the tautomeric forms. The tautomeric equilibrium between thione and thiol tautomers of TCHs extends the conjugation and might provide a structural basis for the excellent radical scavenging ability and antioxidant activity.

The assessment of exact aqueous structure of isomerizable, biologically important molecules is a prerequisite for further drug development. Mass spectrometry studies showed that bis-TCHs might exist as a mixture of two cyclic (2-amino-l,3,4-thiadiazolidine and 1,2,4-triazolidine-3-thione) and one linear form in a gas phase, with the fragmentation peaks corresponding to thiol form. On the other hand, the structure of TCHs in biologically relevant media is not studied in more details. The ^{1}H NMR spectra of the same compounds indicated that only linear, thione form is present in DMSO-d_6 solution [22]. The addition of water into DMSO solution of salicylaldehyde benzoylhydrazone induces the conformational and configurational changes [23].

In this study, we focus on the structural effects responsible for the increased antioxidant potency of TCHs observed upon the addition of water into DMSO solution of compounds. The combination of various spectroscopic techniques and quantum chemical calculations provided the new findings on the isomerism of TCHs in a solution and its impact on antioxidant activity.

Experimental

Materials

Salicylaldehyde, methyl 2-pyridyl ketone, and thiocarbohydrazide (98%) were obtained from Acros Organics (BVBA, Geel, Belgium). All solvents (reagent grade) were obtained from commercial suppliers and used without further purification.

Syntheses of compounds

The compounds **1** [18], **2** [24], **3** [19], and **4** [25] (Fig. 1) have been published earlier. All these compounds are synthesized by literary procedures and their purity was verified through NMR characterization. For the compounds **1** and **3,** there is no complete literary characterization so it is presented in main text, while the characterization of compounds **2** and **4** is given in Electronic Supplementary Material (ESM).

[(*2-hydroxyphenyl*)*methylene*]-*carbonothioic dihydrazide* (**1**)

Yellow solid; Yield 76%; M.p. 186–187 °C; IR (KBr, cm^{-1}) ν_{max}: 3452s (OH), 3196s (NH_2), 3069m (NH), 2999w (CH_{aryl}), 1483s (amide II), 1282vs (C=S); Anal. Calc. For $C_8H_{10}N_4OS$ (210.06 g mol^{-1}): C, 45.70; H, 4.79; N, 26.65; S, 15.25%, Found: C, 45.66; H, 4.77; N, 26.45; S, 15.18%. The solvent for recrystallization: methanol.

E:*Z Isomers ratio* (*81*:*19*). *Isomer E*: ^{1}H NMR (500 MHz, DMSO-d_6, δ ppm): 4.85 (s, 2H, H2–N4); 6.77–6.92 (*m*, 2H, H–C4, H–C6); 7.20 (*t*, 1H, H–C5, $^3J_{5,6}$ = 6.3 Hz); 7.98 (*d*, 1H, H–C3, $^3J_{3,4}$ = 6.5 Hz); 8.33 (s, 1H, H–C7); 9.73 (*s*, 1H, H-C1(OH)); 9.85 (*s*, 1H, H–N3,); 11.35 (s, 1H, H–N2). ^{13}C NMR (126 MHz, DMSO-d_6, δ ppm, TMS): 116.06 (C6); 119.28 (C4); 120.36 (C2); 127.20 (C3); 130.96 (C5); 139.81 (C7); 156.29 (C1); 175.91 (C8); ^{15}N NMR (DMSO-d_6 at 298 K): 96.22 (N4); 133.27 (N3); 166.38 (N2); 310.74 (N1).

Isomer Z: ^{1}H NMR (500 MHz, DMSO-d_6, δ ppm): 4.85 (s, 2H, H2–N4); 6.77-6.92 (*m*, 2H, H–C4, H–C6); 7.26–7.35 (*m*, 1H, H–C3, H-C5); 8.62 (s, 1H, H–C7); 9.28–9.61 ((br.m.ovlp. 2H, H–N3, H-C1(OH)); 11.78 (s, 1H, H–N2). ^{13}C NMR (126 MHz, DMSO-d_6, δ ppm, TMS): 116.06 (C6); 119.28 (C4); 129.25 (C2); 130.30 (C5); 127.61(C3); 147.57 (C7); 155.14 (C1); 171.68 (C8) (ESM, Fig. S1).

E-[*1*-(*2-pyridinyl*)*ethylidene*]-*carbonothioic dihydrazide* (**3**)

Yellow solid; Yield 88%; M.p. 179–181 °C; IR (KBr, cm^{-1}) ν_{max}: 3265 s (NH_2), 3166 m (NH), 3000w (CH_{aryl}), 1500vs (amide II), 1235s (C=S); Anal.Calc. For $C_8H_{11}N_5S$ (209.27 g mol^{-1}): C, 45.91; H, 5.30; N, 33.47; S, 15.32%, Found: C, 45.82; H, 5.21; N, 33.32; S, 15.41%. The solvent for recrystallization: ethanol.

Thione/Thiol form ratio (*97:3*) *Thione form*: ^{1}H NMR (500 MHz, DMSO-d_6, δ ppm): 2.38 (s, 3H, CH_3); 4.98 (s, 2H, H–

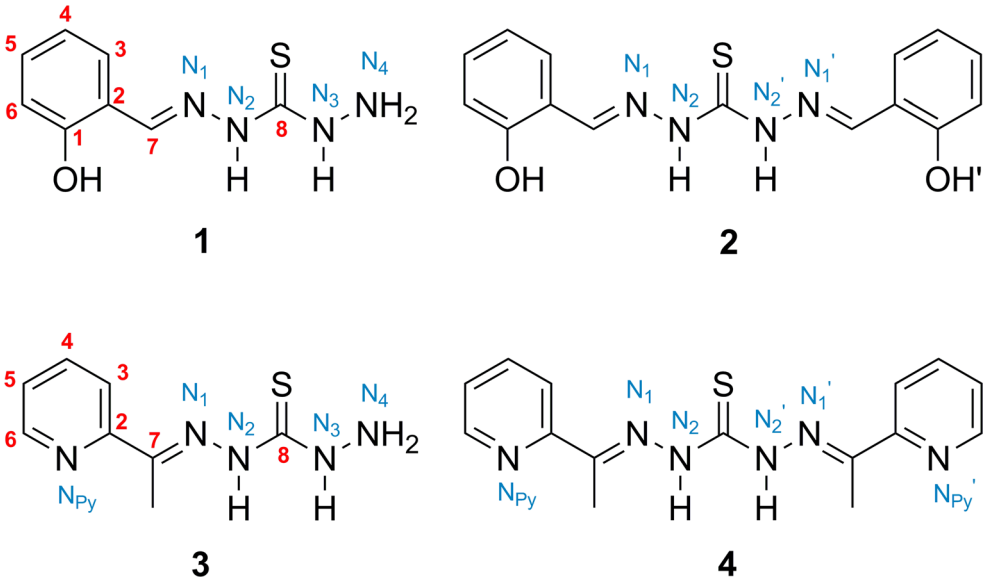

Fig. 1 Structures of investigated mono- and bis-TCHs along with the atom numeration

N4); 7.36 (dd, 1H, H–C5); 7.78 (td, 1H, H–C4, $^{3}J_{4,3}$ = 8.1 Hz); 8.50–8.59 (*m*, 2H, H–C3, H–C6); 9.95 (s, 1H, H-N3); 10.30 (s, 1H, H–N2); ^{13}C NMR (126 MHz, DMSO-d_6, δ ppm, TMS): 12.46 (CH_3); 121.55 (C3); 124.28 (C5); 136.71 (C4); 148.72 (C7); 148.81 (C6); 155.20 (C2); 176.68 (C8); ^{15}N NMR (DMSO-d_6, δ ppm): 72.47 (N4); 136.01 (N3); 162.31 (N2); 310.70 (N_{Ar}); 313.11 (N1).

Thiol form: ^{1}H NMR (500 MHz, DMSO-d_6, δ ppm): 2.37 (3H, CH_3); 4.98 (2H, H–N4); 7.58 (1H, H–C5); 8.08 (1H, H–C4, $^{3}J_{4,3}$ = 8.1 Hz); 8.77 (2H, H–C3, H–C6); 9.54 (s, 1H, H–N3), 14.14 (s, 1H, H–S); ^{13}C NMR (126 MHz, DMSO-d_6, δ ppm, TMS): 23.74 (CH_3); 121.74 (C3); 123.35 (C5); 137.28 (C4); 148.27 (C7); 149.33 (C6); 159.93 (C2); 171.97 (C8) (ESM, Fig. S2).

Free radical scavenging antioxidant assay

The proton donating ability of TCHs was assayed using a protocol for the determination of radical scavenging activity [26]. Compounds were dissolved in DMSO and diluted into ten different concentrations. Commercially available DPPH$^{\cdot}$ (2,2-diphenyl-1-picrylhydrazyl radical) was dissolved in methanol at a concentration of 6.50 × 10^{-5} mol L^{-1}. Into a 96-well microplate, 140 μL of DPPH$^{\cdot}$ solution was loaded and 10 μL DMSO solution of the tested compounds was added, or pure DMSO (10 μL) as the control. The microplate was incubated for 30 min at 298 K in the dark and the absorbance was measured at 517 nm using a Thermo Scientific Appliskan. All the measurements were carried out in triplicate. The scavenging activity of the compounds was calculated using Eq. (1):

$$\text{Scavenging activity}\ (\%) = \frac{\left(A_{\text{control}} - A_{\text{sample}}\right)}{A_{\text{control}}} \times 100 \qquad (1)$$

where A_{sample} and A_{control} refer to the absorbances at 517 nm of DPPH$^{\cdot}$ in the sample and control solutions, respectively.

IC_{50} values were calculated from the plotted graph of scavenging activity against the concentrations of the samples. IC_{50} is defined as the total antioxidant concentration necessary to decrease the amount of the initial DPPH$^{\cdot}$ by 50%. IC_{50} was calculated for all compounds based on the percentage of DPPH$^{\cdot}$ scavenged. Ascorbic acid was used as the reference compound (positive control) with concentrations from 50 to 500 mg L^{-1}.

Samples preparation for UV measurements

Stock solutions of all compounds were prepared by dissolution of the weighed samples in DMSO. The working solutions was prepared in a 10.0 mL volumetric flask by adding appropriate volume of stock solution and water, and diluted to 10.0 mL with DMSO. Working sample, used for the measurement of UV–Vis spectra, was prepared in a such a way to obtain V(DMSO)/V(H_2O) mixed solvents ratio of 4/1 [27] (Fig. 2). Concentration of compound in the obtained solution was 5 × 10^{-5} mol L^{-1}.

Physical measurements

Elemental analyses (C, H, N) were performed by the standard micromethods using the ELEMENTAR Vario ELIII C.H.N.S=O analyzer.

Fourier-transform infrared (FTIR) spectra were obtained using FTIR BOMEM MB 100 in the form of KBr pellets. FTIR spectra were recorded in the transmission mode between 400 and 4000 cm^{-1} with a resolution of 4 cm^{-1}. Abbreviations used for IR spectra are as follows: vs, very strong; s, strong; m, medium; w, weak.

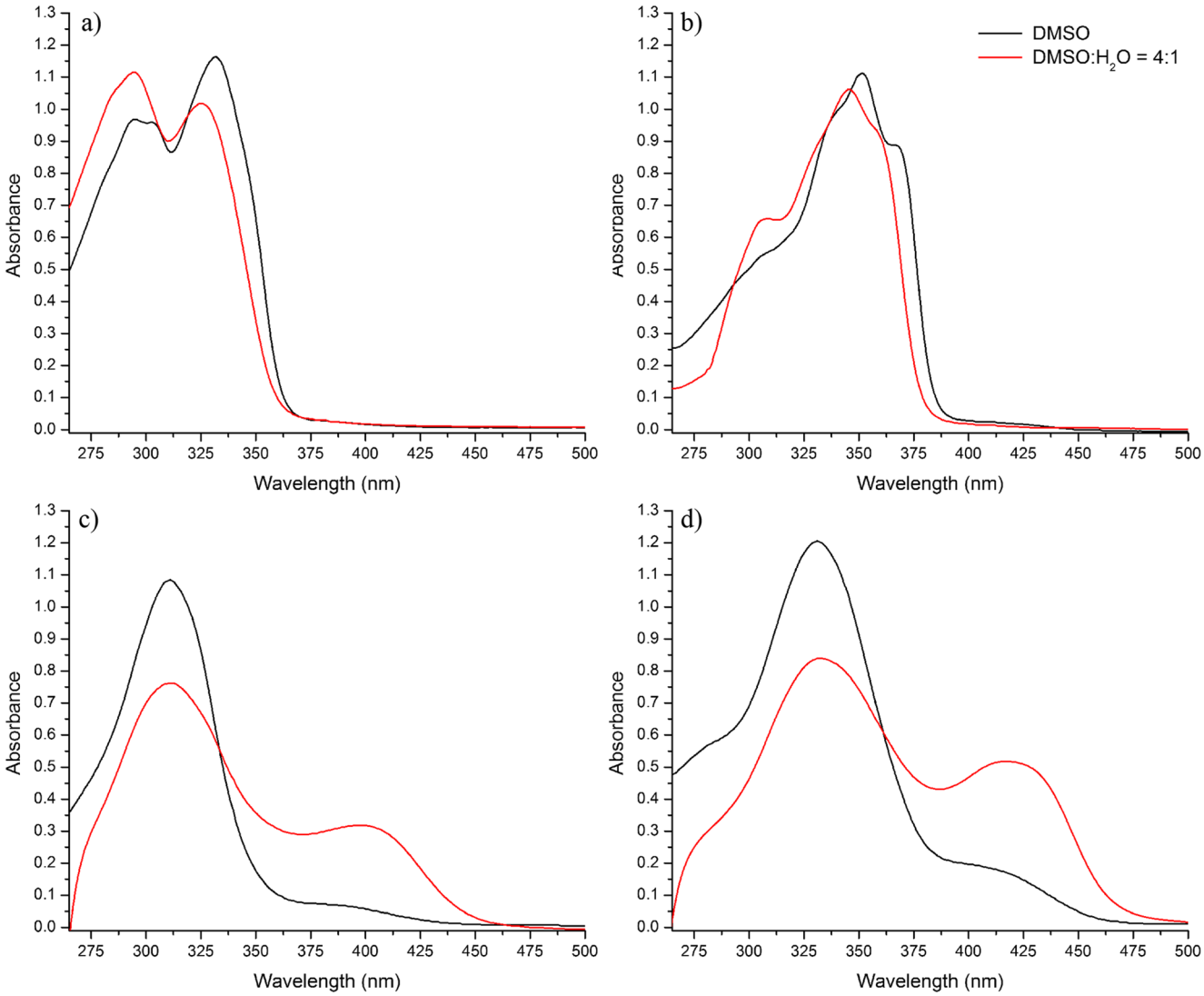

Fig. 2 The UV/Vis spectra changes induced by the addition of water in the DMSO solution of **a) 1**; **b) 2**; **c) 3**; **d) 4**

NMR spectral assignments and structural parameters were obtained by combined use of 1D (^{1}H and ^{13}C, Figs. S3–S10) and 2D (COSY, NOESY, ^{1}H-^{13}C HSQC, and ^{1}H-^{13}C HMBC) spectra are given in ESM, Figs. S11–S24. The NMR spectra were recorded on Bruker Avance 500 equipped with broad-band direct probe. Chemical shifts are given on δ scale relative to tetramethylsilane (TMS) as an internal standard for ^{1}H and ^{13}C. Abbreviations used for NMR spectra are as follows: s, singlet; dd, doublet of doublets; ddd, double double doublet.

Computational chemistry studies

The initial geometry of each isomeric form was obtained using MMFF94 force field [28]. Afterward, conformational seach was performed using AMMP program [29] and Vega ZZ 3.1.0 GUI [30]. Boltzman jump search parameters were used, while all flexible torsions were rotated by 15°. Dielectric constant was set to 78.4 (water) and other settings were retained at default values. The lowest energy conformer of each form was additionally optimized using DFT with B3LYP functional and 6-311++G(d,p) basis set. Non-specific solvent effects were simulated using the water IEF-PCM model. Frequency calculations were performed in order to obtain zero-point corrected energies and other thermodynamic parameters. No imaginary vibrational frequencies were present in the optimized geometries, confirming that the geometry reported represent the minimum on the potential energy surface. The absorption spectra are simulated using time-dependent DFT method with CAM-B3LYP functional [31] and the same basis set as for geometry optimization, while solvent effects were simulated using IEF-PCM model of DMSO. Gauge independent atomic orbital (GIAO) method [32] was used for predicting the NMR chemical shifts of diastereoisomers in DMSO. The rotational barrier was calculated by stepwise rotation around C_2–C_7 bond by 20° and geometry optimization of each rotamer at DFT/ωB97XD/6-311g(d,p) level to account

for dispersion interactions [33]. All calculations were performed in Gaussian09 [34].

Results and discussion

The antioxidant activity of TCHs and the water-induced structural changes

It is known that thione antioxidants, such as ergothioneine [35] and thiosemicarbazones [36, 37], show good free-radical scavenging activities. In this study, antioxidant activity of four TCHs (Fig. 1) was analyzed using a DPPH method [26].

Mono- and bis-TCHs with 2-hydroxyphenyl group on azomethine carbon (comps. **1** and **2**) were better DPPH$^{\cdot}$ scavengers than compounds bearing 2-acetylpyridine moiety (**3** and **4**) (Table 1). Generally, the presence of hydroxyl groups increases the antioxidant activity of TCHs [7].

Interestingly, it was observed that the addition of 20% water in DMSO solution of DPPH$^{\cdot}$ increase the antioxidant activity of the investigated compounds (Table 1). To explain this phenomenon, we performed structural investigation of studied molecules to get the fundamental information necessary for establishing the structure-property relationships. Two possible structural changes are hypothesized: *E*/*Z* isomerism around imine bond and thione/thiol tautomerism.

E/*Z* isomers around imine bond(s) can contribute to diverse chelating properties as well as pharmacodynamics profiles [38]. Thione-thiol tautomerism is also important for the biological activity of compounds as different tautomers have different ADMET properties as well as different hydrogen bonding preferences in the interaction with the biological targets [39]. To further characterize the solution structure of studied compounds, *E*/*Z* isomerization, as well as thione-thiol tautomerism were examined in DMSO/water mixtures and discussed with the aid of quantum chemical calculations.

A variety of spectroscopic methods could be used for analysis of the state of tautomeric equilibria, *i.e.*, study of the mechanism of tautomer/isomer transformation. Absorption spectra of isomers/tautomers are generally different and could be useful for detection/quantification of solvent induced isomerization/tautomerization [40]. For structurally related aroylhydrazones, it has been reported that one type of isomer prevails in non-aqueous media, while water induces isomerization into another configurational isomer [41]. It was shown that *E*/*Z* photoisomerization of pyridine-substituted semicarbazide Schiff bases is followed by a red shift of the absorption maximum [42, 43]. Also, the addition of water could support the tautomeric conversion of the existing geometric isomers, as reported for structurally similar thionamide/thiolimine isomerization [44].

Table 1 Antioxidant activities of mono- and bis-TCHs, determined in the DPPH assay and expressed as IC_{50} values (in mM)

	IC_{50} (DMSO)	IC_{50} (DMSO:H_2O = 4:1)
1	0.15	0.083
2	0.13	0.078
3	0.24	0.11
4	0.67	0.13
Ascorbic acid	0.11	0.21

In order to analyze water-induced structural changes, the electronic absorption spectra of four TCHs (Fig. 1) were recorded in DMSO and DMSO/water mixture. The obtained spectra (Fig. 2) show the changes in the position and intensity of absorption peaks, *i.e.*, solvent induced *E*/*Z* isomerization or thione-thiol tautomeric equilibria shift, with the addition of water in DMSO solution of TCHs. Water-induced formation of thiolimine tautomer is usually accompanied by the appearance of a new band at ~ 400 nm [44], while *E*/*Z*-photoisomerization also causes the red-shift of the absorption maximum [42, 43]. Therefore, based only on UV–Vis spectra of the investigated compounds, it is very difficult to elucidate which of these two phenomena occurs.

^{1}H NMR experiments were useful for resolving this uncertainty. The spectra of **1** and **2** in DMSO-d_6/H_2O mixture didn't show a characteristic downfielded signal for iminothiolic SH group at ~ 15 ppm [10], excluding the possibility for thione/thiol (thioamide-iminothiol) tautomerism (ESM, Figs. S3 and S4). Based on these experiments, it was concluded that **1** and **2** undergo *E*/*Z* isomerization upon addition of water in the DMSO solution.

The possible mechanism on water induced *E*-to-*Z* isomerization is hypothesized. The addition of water in DMSO solution might destabilize the ground state of **1** by disturbing the intramolecular hydrogen bond, thereby reducing the energy barrier for *E*-to-*Z* isomerization (ESM, Fig. S1). The ^{1}H NMR spectroscopy supports this hypothesis, as the peak at 11.73 ppm, which is assigned to *Z*-isomer, increases while simultaneously the peak of *E*-isomer at 11.37 ppm decreases (ESM, Fig. S3). After the addition of water, the *E*/*Z* ratio is changed from 81:19 to 21:79. Literature describes that ^{1}H NMR chemical shifts of N_2–H proton of structurally similar thiosemicarbazones move downfield by 0.22 ppm upon UV irradiation, as a consequence of *E*/*Z* photoisomerization [42]. The preference of **1** toward *E*-configuration was assessed by 2D NOESY spectrum, showing through-space correlations between H-atoms at C_7/C_3 and OH/N_3-H (ESM, Fig. S14).

Although being symmetrical, **2** shows two distinct ^{1}H NMR signals for both hydrazide and imine nitrogen protons (ESM, Fig. S4a). The presence of two distinct signals for NH protons was already reported for bis(hydrazones) [25]. The addition of water into DMSO solution of **2** induces smaller changes in UV–Vis spectrum (Fig. 2b). Two ^{1}H NMR signals originating

from N_2–H and N_2'–H at 12.10 and 11.92 ppm (ESM, Fig. S4a) merged upon the addition of H_2O, and the intensity of new peak corresponds to two protons (ESM, Fig. S4b).

In order to explain this effect, we predicted the ^{1}H NMR shifts for (*E*,*E*)-, (*E*,*Z*)- and (*Z*,*Z*)-forms of **2** using GIAO method. The difference in chemical shifts of N_2–H and N_2'–H (Δ_δ) (Fig. 1) decreases from 0.97 to 0.17 ppm upon (*E*,*E*)- to (*E*,*Z*)-isomerization (ESM, Table S1), while complete transition to (*Z*,*Z*)-isomer yields a symmetrical structure with negligible $\Delta\delta$ value of 0.01 ppm. Therefore, the observed overlapping of two N–H peaks in ^{1}H NMR spectrum (ESM, Figs. S4a and S4b) might originate from *E*-to-*Z* isomerization.

According to ^{1}H NMR spectra, the compound **2** is present in a solution as **2**-(*E*,*Z*) form in DMSO, and upon addition of water the equilibrium shifts to **2**-(*Z*,*Z*) form. The small percentage of water, present in a hygroscopic DMSO-d_6, might be enough to initialize the **2**-(*E*,*E*) to **2**-(*E*,*Z*) isomerization to some extent. ^{13}C-NMR spectrum of compound **2** showed two signals of olefinic carbons, suggesting the existence of two diastereomeric carbazone moieties (ESM, Fig. S8) and further confirming the presence of **2**-(*E*,*Z*) isomer in a solution. In addition, correlation between H-atoms at N_2 and N_2' in the NOESY spectrum of **2** (ESM, Fig. S17), which may be present only in the case of the *E*/*Z* and the *Z*/*Z* isomers (ESM, Table S1), additionally confirms this claim.

On the contrary, compound **4** showed symmetric structure and no diastereomeric moieties were recognized in its ^{13}C-NMR spectrum (ESM, Figs. S10 and S22). ^{1}H NMR data suggest a symmetric structure in which the C=S bond is located on the symmetry line of the molecule (ESM, Fig. S6). It could be supposed that the methyl groups limit the flexibility of a molecule by increasing the energy barrier for isomerization, so it preferentially adopts a symmetric conformation [25].

Although **1** and **2** exhibits *E*/*Z* isomerization, compounds **3** and **4** undergo thione/thiol tautomerism upon the addition of water. This is confirmed by the appearance of highly downfield signal characteristic for –SH proton in ^{1}H NMR spectrum (14.14 and 15.41 ppm, ESM, Figs. S5a and S6a) [10, 45]. The *E*- and (*E*/*E*)-configuration of hydrazone moiety in compounds **3** and **4** can be evidenced by NOESY cross-correlations of H-atoms from -CH_3 and N_2-H (ESM, Figs. S21 and S24). Furthermore, the absence of through-space correlation between H-atoms at -CH_3 and C_3-H which is expected for *Z*-isomer (ESM, Fig. S2; 3-b-*Z* form) further confirms the claim.

The *E*-to-*Z* isomerization around C=N double bond can proceed *via* two mechanisms: torsional route around C=N bond and *in-plane* inversion, where the transition state has a linear geometry with N atom being *sp* hybridized [46]. As torsional pathway cannot be omitted from the considerations on possible isomerization mechanisms [47], it is likely that the torsional route is a preferential mechanism for *E*/*Z* isomerization of TCHs, similar to azobenzene [46]. In sterically congested systems, *E*/*Z* isomerization via torsional route is hindered. This might explain the observed *E*/*Z* isomerization in **1** and **2**, and the lack of isomerization in sterically more demanding **3** and **4**.

After the addition of water to DMSO solution of **3** and **4**, the proportion of thiol form increases. The intensity of corresponding ^{1}H NMR signals increased from 0.03 to 0.18 for **3** (ESM, Fig. S5), and from 0.17 to 0.35 in case of **4** (ESM, Fig. S6), which means that the ratio of thione/thiol forms is changed from 97:3 to 85:15 for compound **3**, and from 85:15 to 66:35 for compound **4**.

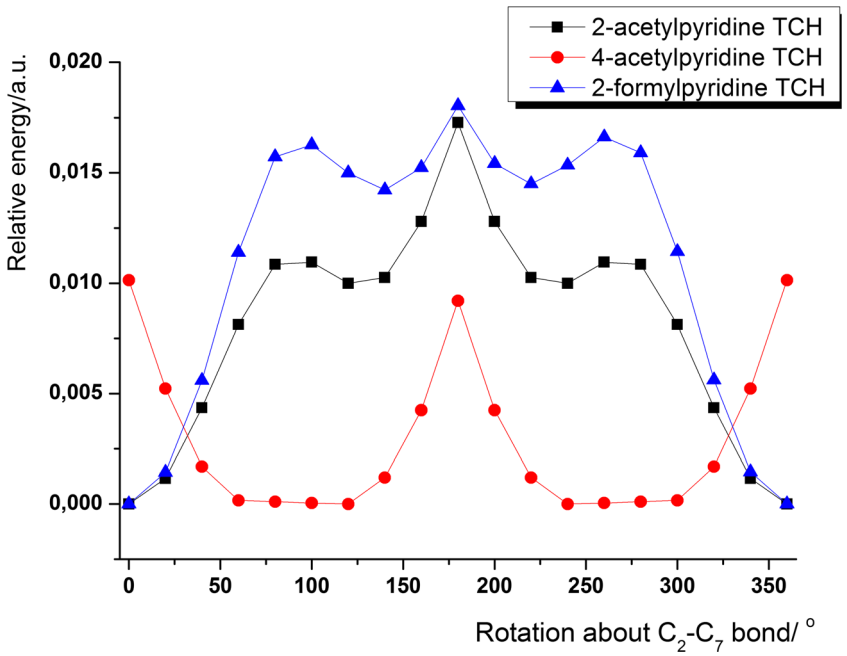

Fig. 3 Graphical presentation of relative energy of comp. **3** and two structural analogs *versus* stepwise rotation around C_2–C_7 bond, in respect to the most stable rotamer

Additionally, a new absorption maximum appears in the UV–Vis spectra at 400 nm for **3** (Fig. 2c) and 425 nm for **4** (Fig. 2d). In the simulated UV–Vis spectra of **4**, the absorption maximum of thiol form is red-shifted by ~ 20 nm compared to thione, and additional peak appears at ~ 270 nm (ESM, Fig. S25).

The water-induced thione/thiol tautomerization is more pronounced in **4** (NMR signal ratio of *E*-thione:thiol is 1:0.35) compared to **3** (*E*-thione:thiol 1:0.18). This result enforces the significance of hydrogen bonding established by intermolecular solvent/solute interactions, which prevail over intramolecular H-bond (IHB) in a cyclic structure of **3-***Z* form (ESM, Fig. S2; 3-b-*Z* form). Although the strong IHB observed in *Z*-isomers of bis(2-pyridil)hydrazones [15] yields a highly downfield ^{1}H NMR signal at ~ 15 ppm, the signal observed in the NMR spectra of **3** and **4** does not originate from intramolecularly bonded N_2–H but from thiolic –SH atom.

To evaluate the relative strength of IHB in compound **3** (2-acetylpyridyl TCH) and sterically less hindered 2-formylpyridyl derivative, the rotational barriers for the rotation of pyridine ring around thiocarbohydrazide moiety are calculated at DFT/ωB97XD/6-311g(d,p) level. To quantify the sterical contribution to the overall rotational barrier of **3**, a hypothetical derivative with pyridine N atom at position 4 is also considered.

The relative energies of comp. **3** and two structural analogs, i.e., mono-TCHs based on 4-acetylpyridine (4-ap; (*Z*)-[1-(4-pyridinyl)ethylidene]carbonothioic dihydrazide) and 2-formylpyridine (2-fp; ((*Z*)-(2-pyridinylmethylene)carbonothioic dihydrazide), were comparatively analyzed with respect to stepwise change of rotation around C_2–C_7, i.e., torsional angle change. Obtained results are presented in Fig. 3.

Table 2 The zero-point corrected energy and enthalpy of **1**–**4** in different configurational/tautomeric forms. The bond dissociation enthalpies for corresponding X–H bonds are shown. The percentage of spin delocalization is reported, calculated as 1–*spin located at heteroatom* which remained after geometry optimization of a radical

	E, Hartree*	*H*, Hartree	BDE (kcal/mol)	% of spin delocalized
1-*E***	− 1003.280812	− 1003.266216		
1-*E* O˙	− 1002.645219	− 1002.630606	85.14	68.5
1-*E* N_2˙	− 1002.643755	− 1002.630212	85.39	53.9
1-*E* N_3˙	− 1002.661405	− 1002.647469	74.56	65.2
1-*E* N_4˙	− 1002.651313	− 1002.637514	80.81	22.1
1-*Z*	− 1003.258467	− 1003.243658		
1-*Z* O˙	− 1002.639390	− 1002.625150	74.41	70.9
1-*Z* N_2˙	− 1002.629226	− 1002.615147	80.69	51.7
1-*Z* N_3˙	− 1002.644748	− 1002.630488	71.06	64.1
1-*Z* N_4˙	− 1002.630368	− 1002.616346	79.94	24.1
2-(*E*,*E*)	− 1347.665656	− 1347.645320		
2-(*E*,*E*) O˙	− 1347.024326	− 1347.003802	88.85	67.0
2-(*E*,*E*) N˙	− 1347.031306	− 1347.011300	84.15	54.8
2-(*Z*,*Z*)	− 1347.629283	− 1347.608459		
2-(*Z*,*Z*) O˙	− 1346.998695	− 1346.978125	81.83	66.1
2-(*Z*,*Z*) N˙	− 1347.003122	− 1346.982485	79.10	55.0
3-*thione***	− 983.385815	− 983.370732		
3-*thione* N_2˙	− 982.746778	− 982.731858	87.19	51.5
3-*thione* N_3˙	− 982.762078	− 982.747400	77.44	65.7
3-*thione* N_4˙	− 982.757113	− 982.742808	80.32	23.1
3-*thiol*	− 983.366585	− 983.351654		
3-*thiol* S˙	− 982.733342	− 982.718097	80.68	20.6
3-*thiol* N_3˙	− 982.749506	− 982.734528	70.54	63.5
3-*thiol* N_4˙	− 982.738845	− 982.723987	77.23	26.8
4-*thione*	− 1307.871753	− 1307.850203		
4-*thione* N_2˙	− 1307.233272	− 1307.211542	87.06	57.0
4-*thiol*	− 1307.852979	− 1307.830817		
4-*thiol* S˙	− 1307.222336	− 1307.200584	81.77	18.2
4-*thiol* N_2˙	− 1307.225046	− 1307.202900	80.32	52.2

*Energies are zero-point energy corrected; **compounds **1** and **2** are modeled as thione tautomers; ***compounds **3** and **4** are modeled in all-*E* configuration

The higher stability of planar structure was obtained for 2-fp and 2-ap TCH, where IHB was formed. Oppositely, steric repulsion in TCH based on 4-ap means higher energy and rotation for 60° bring to structure with minimum energy. Also, obtained results indicate weaker IHB in comp. **3** than in TCH based on 2-fp, with local maxima at 90° rotation corresponding to energy necessary for hydrogen bond breakage. Somewhat higher energy is necessary for hydrogen bond breakage in TCH based on 2-fp due to stronger IHB, where larger steric interference in comp. **3** cause decrease of relative energy. Overall relative energy for both TCHs based on 2-fp and 2-ap are similar at 180° rotation as steric component is more pronounced for 2-ap compared to 2-fp derivatives. In general, weaker IHB was obtained for comps. **3** than for sterically less hindered TCH based on 2-fp. This claim is in line with hydrogen bond formation of (*Z*)-(2-pyridinyl)-based carbonic dihydrazide, where the presence of the methyl group on azomethine carbon, instead of hydrogen atom, reduces the IHB ability [14].

The effect of configurational isomerism and thione/thiol tautomerism on the increase of antioxidant activity of TCHs

Aiming to explain how water-induced structural changes improve the antioxidant activity of TCHs, we performed detailed electronic structure and bond dissociation enthalpy (BDE) calculations. The radical scavenging ability of a molecule (M–H) is associated with the ability to transfer H atom to any free radical (for example $DPPH^{\cdot}$), as shown by the reaction:

$$M\text{–}H + DPPH^{\cdot} \rightarrow M^{\cdot} + DPPH_2$$

Among many potential mechanisms of this process (HAT, hydrogen atom transfer; SET, single-electron transfer; SPLET, sequential proton loss electron transfer), the HAT is the simplest and most widely studied one. The HAT potency of a compound is determined by the BDE of molecule, where H atom of the most labile X–H bond (where X can be any heteroatom) will be abstracted first. The BDE value can be calculated by the equation:

$$\mathrm{BDE\ (M\text{–}H)} = \Delta_f H(M^{\cdot}) + \Delta_f H(H) - \Delta_f H(MH), \qquad (2)$$

where $\Delta_f H(M^{\cdot})$ is the enthalpy of formation (EOF) of the radical formed by hydrogen atom abstraction, $\Delta_f H(H)$ is the EOF of hydrogen atom, and $\Delta_f H(MH)$ is the EOF of a molecule. The stabilization of radical species by the resonance, conjugation, and intramolecular hydrogen bonding leads to the lower values for BDE, and is usually followed by the increased *in vitro* antioxidant activity [48].

The relative stability of *E*- and *Z*-isomers of both thione and thiol tautomers of compounds **1** and **3** was studied by quantum chemical calculations at DFT/B3LYP/6-311++G(d,p) level using IEF-PCM model of water. The results obtained (ESM, Figs. S27 and S28) may serve only for qualitative purpose as PCM model do not account for explicit hydrogen bonding between solvent and solute. Such explicit interactions may play a significant role in lowering/increasing the energy barrier for isomerization or tautomerization.

The most stable isomer of **1** appeared to be the **1**-*E*-thione form (ESM, Fig. S27). *E*-to-*Z* isomerism breaks the pseudo 6-membered ring formed by intramolecular hydrogen bonding between the –OH group and N_1 atom. The *E*-thione form was

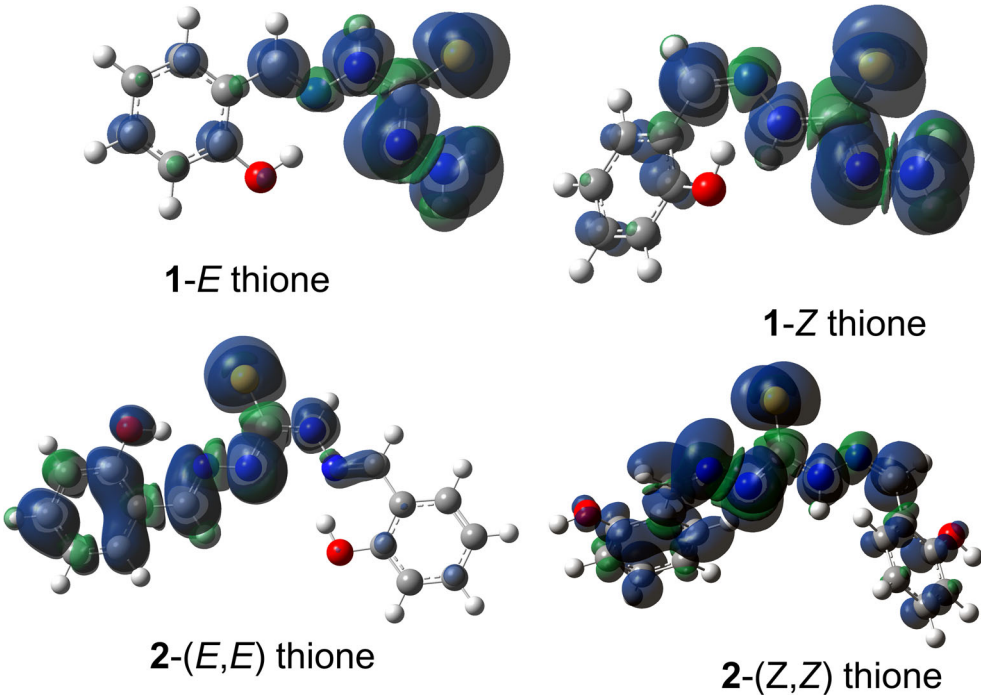

Fig. 4 Spin density distribution for radicals formed by hydrogen atom abstraction from the lowest energy N–H bond in **1** and **2**

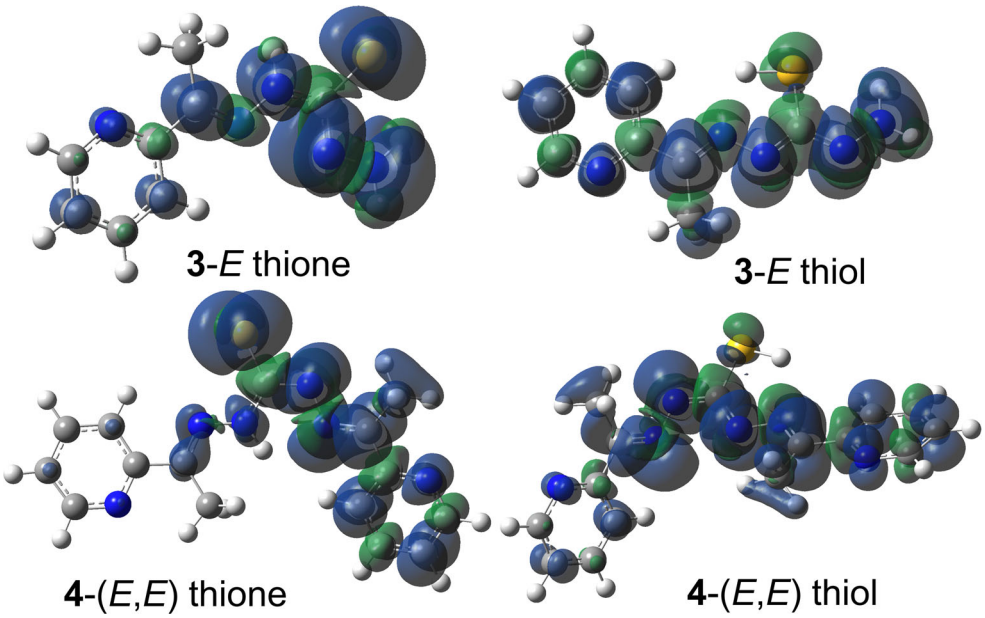

Fig. 5 Spin density distribution of radicals formed by HAT from N_3–H bond of **3**-*E* and N_2–H bonds of **4**-(*E*,*E*) isomers, for both thione and thiol tautomers

also the most stable form for compound **3**, although the intramolecular H-bond between the N_2–H and N_{Py} apparently decreases the energy difference between two geometric isomers (ESM, Fig. S28).

As the addition of water induces *E*/*Z* isomerization of **1** and almost halve the IC_{50} values toward DPPH$^{\cdot}$ (Table 1), we performed BDE calculations to see if the appearance of *Z*-isomer facilitates the HAT. Both **1**-*E* and **1**-*Z* isomers were modeled in thione tautomeric form. As can be seen from Table 2, *Z*-isomers have 3-5 kcal/mol lower BDEs of –N–H atoms attached to C=S (–N_3–H and –N_2–H), while isomerization does not influence the BDE of terminal –NH_2 group (–N_4–H). The most striking difference is observed for –OH group, where *E*/*Z* isomerization decreased the BDE by 11 kcal/mol. Upon isomerization to *Z*-isomer, the phenolic –OH group is released from intramolecular hydrogen-bonded 6-membered ring. This effect makes the –OH group more prone to interaction with DPPH$^{\cdot}$, while ground state destabilization decreases the BDE (Eq. (2)) and facilitates HAT.

The isomerization of **2** from *E*,*E* to *Z*-*Z* decreases the BDE of O and N_3 radicals by ~ 7 and 5 kcal/mol, respectively (Table 2).

Spin density distribution map helps visualizing the extent of spin delocalization, which influences the overall stability of a radical formed by HAT. The spin density distribution of O (Fig. S29) and N-radicals (Fig. 4) of **1**-*Z* and **2**-(*Z*,*Z*) forms is more delocalized compared to *E*-isomers. The additional spin delocalization corroborates with the increased radical scavenging potency upon isomerization.

In order to study the influence of thione/thiol tautomerism on antioxidant activity of **3**, the BDEs of several bonds were calculated for thione and thiol tautomers, starting from *E*-geometry. Thione/thiol tautomerism decreases the lowest BDE by 7 kcal/mol (Table 2), supporting the trends in experimentally obtained antioxidant activities.

Although one may expect –SH group as the most probable site for interaction with DPPH$^{\cdot}$, we found that –N_3-H bond of **3** is more labile, with ~ 10 kcal/mol lower BDE (Table 2). To see if such a trend is maintained for bis-derivative, we performed BDE calculations for compound **4**. The BDE of –N_2–H bond of (*E*,*E*)-thione form was 87.06 kcal/mol. Isomerization to (*E*,*E*)- thiol form decreased the BDE of –N_2–H to 80.32 kcal/mol, while –SH had a similar BDE value (81.77 kcal/mol). The presence of two almost equally reactive sites should lead to the increase of the antioxidant potency of **4**, and this effect explains the 5-fold drop in the IC_{50} values upon the addition of water (from 0.67 to 0.13 mM, Table 1).

As can be seen from Fig. 5, thiol form of **3** and **4** has more delocalized spin which stabilizes the radical species, decreases the corresponding BDE, and finally increases the antioxidant activity.

Conclusion

In conclusion, the presence of hydroxyl groups increases the antioxidant activity of TCHs as **1** and **2** were more potent radical scavengers compared to 2-acetylpyridine analogs **3** and **4**. The addition of water affects the intramolecular hydrogen bond strength in **1**-*E* form facilitating *E*-to-*Z* isomerization, and thus increases the antioxidant activity due to formation of "free" –OH group in **1**-*Z* isomer with 11 kcal/mol lower BDE. Electron spin delocalization is more pronounced in *Z*-isomers of **1** and **2**.

The addition of water into DMSO solution of **3** and **4** causes thione-to-thiol tautomerization, as seen from the

appearance of red-shifted UV–Vis absorption maximum and a deshielded ^{1}H NMR signal of –SH proton. The presence of thiol form in a solution is correlated with the increase in antioxidant activity. Two low-energy bonds of **4** (–N–H and –S–H) along with the delocalized spin density of thiol radical rationalize the observed increase in the radical scavenging activity.

The results of this study provide new insights on the solution structure of TCHs as biologically active compounds, and also highlight the importance of detailed structural characterization in studying structure-antioxidant relationships of TCHs or other isomerizable compounds.

Funding information The Ministry of Education, Science and Technological Development of the Republic of Serbia supported this work, Grant Nos. 172013, 172035, and 172055, and represents the part of the bilateral project between Serbia and Montenegro titled "Synthesis of Schiff bases and investigation of their antimicrobial and antioxidant activity."

Compliance with ethical standards

Conflict of interest The authors declare that they have no conflict of interest.

References

1. Kaya Y, Erçağ A, Kaya K (2018). J Coord Chem 71:3364–3380
2. Božić AR, Bjelogrlić SK, Novaković IT, Filipović NR, Petrović PM, Marinković AD, Todorović TR, Cvijetić IN (2018). ChemistrySelect 3:2215–2221
3. Hameed A, al-Rashida M, Uroos M, Abid Ali S, Khan KM (2017). Expert Opin Ther Pat 27:63–79
4. Whitnall M, Howard J, Ponka P, Richardson DR (2006). Proc Natl Acad Sci U S A 103:14901–14906
5. Richardson DR, Kalinowski DS, Richardson V, Sharpe PC, Lovejoy DB, Islam M, Bernhardt PV (2009). J Med Chem 52: 1459–1470
6. Nutting CM, van Herpen CML, Miah AB, Bhide SA, Machiels J-P, Buter J, Kelly C, de Raucourt D, Harrington KJ (2009). Ann Oncol 20:1275–1279
7. Božić A, Marinković A, Bjelogrlić S, Todorović TR, Cvijetić IN, Novaković I, Muller CD, Filipović NR (2016). RSC Adv 6: 104763–104781
8. Bavin EM, Rees RJW, Robson JM, Seiler M, Seymour DE, Suddaby D (1950) The tuberculostatic activity of some thiosemicarbazones. J Pharm Pharmacol 2:764–772
9. Pirrung MC, Pansare SV, Das SK, Keith KA, Kern ER (2005). J Med Chem 48:3045–3050
10. Abu El-Reash GM, El-Gammal OA, Radwan AH (2014). Spectrochim Acta A Mol Biomol Spectrosc 121:259–267
11. Dragancea D, Shova S, Enyedy ÉA, Breza M, Rapta P, Carrella LM, Rentschler E, Dobrov A, Arion VB (2014). Polyhedron 80: 180–192
12. Tiwari ADD, Mishra AKK, Mishra SBB, Mamba BBB, Maji B, Bhattacharya S (2011). Spectrochim Acta A Mol Biomol Spectrosc 79:1050–1056
13. Bozic A, Filipovic N, Novakovic I, Bjelogrlic S, Nikolic J, Drmanic S, Marinkovic A (2017). J Serb Chem Soc 82:495–508
14. Božić AR, Filipović NR, Verbić T, Milčić MK, Todorović TR, Cvijetić IN, Klisurić OR, Radišić MM, Marinković AD (2017). Arab J Chem. https://doi.org/10.1016/j.arabjc.2017.08.010
15. Gordillo MA, Soto-Monsalve M, Carmona-Vargas CC, Gutiérrez G, D'vries RF, Lehn J-M, Chaur MN (2017). Chem Eur J 23: 14872–14882
16. Bacchi A, Carcelli M, Pelagatti P, Pelizzi C, Pelizzi G, Zani F (1999). J Inorg Biochem 75:123–133
17. Al-Omair MA, Sayed AR, Youssef MM (2015). Molecules 20: 2591–2610
18. Shi Z, Zhao Z, Liu M, Wang X (2013). CR Chim 16:977–984
19. Bacchi A, Bonini A, Carcelli M, Ferraro F, Leporati E, Pelizzi C, Pelizzi G (1996) J Chem Soc Dalton Trans 2699–2704
20. Nasr T, Bondock S, Eid S (2014). Eur J Med Chem 84:491–504
21. Peerannawar S, Horton W, Kokel A, Török F, Török M, Török B (2017). Struct Chem 28:391–402
22. Lashin VV, Terent'ev PB, Zelenin KN, Bulakhov GA, Alekseev VV (1994). Chem Heterocycl Compd 30:498–500
23. Cordier C, Vauthier E, Adenier A, Lu Y, Massat A, Cossé-Barbi A (2004). Struct Chem 15:295–307
24. Maity D, Manna AK, Karthigeyan D, Kundu TK, Pati SK, Govindaraju T (2011). Chem Eur J 17:11152–11161
25. Ebrahim Tehrani KHM, Kobarfard F, Azerang P, Mehravar M, Soleimani Z, Ghavami G, Sardari S (2013). Iran J Pharm Res 12: 331–346
26. Prior RL, Wu X, Schaich K (2005). J Agric Food Chem 53:4290–4302
27. Galić N, Dijanošić A, Kontrec D, Miljanić S (2012). Spectrochim Acta A Mol Biomol Spectrosc 95:347–353
28. Halgren TA (1999). J Comput Chem 20:720–729
29. Harrison RW (1993). J Comput Chem 14:1112–1122
30. Pedretti A, Villa L, Vistoli G (2004). J Comput Aided Mol Des 18: 167–173
31. Yanai T, Tew DP, Handy NC (2004). Chem Phys Lett 393:51–57
32. Wolinski K, Hinton JF, Pulay P (1990). J Am Chem Soc 112:8251–8260
33. Chai J-D, Head-Gordon M (2008). Phys Chem Chem Phys 10: 6615–6620
34. Frisch MJ, Trucks GW, Schlegel HB, Scuseria GE, Robb MA, Cheeseman JR, Scalmani G, Barone V, Mennucci B, Petersson GA, Nakatsuji H, Caricato M, Li X, Hratchian HP, Izmaylov AF, Bloino J, Zheng G, Sonnenberg JL, Hada M, Ehara M, Toyota K, Fukuda R, Hasegawa J, Ishida M, Nakajima T, Honda Y, Kitao O, Nakai H, Vreven T, Montgomery JA, Peralta JE, Ogliaro F, Bearpark M, Heyd JJ, Brothers E, Kudin KN, Staroverov VN, Kobayashi R, Normand J, Raghavachari K, Rendell A, Burant JC, Iyengar SS, Tomasi J, Cossi M, Rega N, Millam JM, Klene M, Knox JE, Cross JB, Bakken V, Adamo C, Jaramillo J, Gomperts R, Stratmann RE, Yazyev O, Austin AJ, Cammi R, Pomelli C, Ochterski JW, Martin RL, Morokuma K, Zakrzewski VG, Voth GA, Salvador P, Dannenberg JJ, Dapprich S, Daniels AD, Farkas Ö, Foresman JB, Ortiz JV, Cioslowski J, Fox DJ (2009) Gaussian 09, Revis. B.01. Gaussian, Inc., Wallingford
35. Cheah IK, Halliwell B (2012) Ergothioneine; antioxidant potential, physiological function and role in disease. BBA–Mol Basis Dis 1822:784–793
36. Zimmerman MT, Bayse CA, Ramoutar RR, Brumaghim JL (2015). J Inorg Biochem 145:30–40
37. Calcatierra V, López Ó, Fernández-Bolaños JG, Plata GB, Padrón JM (2015). Eur J Med Chem 94:63–72
38. Kovaříková P, Vávrová K, Tomalová K, Schöngut M, Hrušková K, Hašková P, Klimeš J (2008). J Pharm Biomed Anal 48:295–302
39. Milletti F, Vulpetti A (2010). J Chem Inf Model 50:1062–1074
40. Fabian WMF, Antonov L, Nedeltcheva D, Kamounah FS, Taylor PJ (2004). J Phys Chem A 108:7603–7612

41. Kuodis Z, Rutavičius A, Matijoška A, Eicher-Lorka O (2007). Cent Eur J Chem 5:996–1006
42. Lin L, Fan W, Chen S, Ma J, Hu W, Lin Y, Zhang H, Huang R (2012). New J Chem 36:2562–2567
43. Uchiyama S, Ando M, Aoyagi S (2003). J Chromatogr A 996:95–102
44. Galić N, Cimerman Z, Tomišić V (2008). Spectrochim Acta A Mol Biomol Spectrosc 71:1274–1280
45. The ^{1}H NMR spectrum of 1H-1,2,4-triazole-3-thiol; https://sdbs.db.aist.go.jp, SDBS No. 22953, Accessed 18 March 2019
46. Gagliardi L, Garavelli M, Orlandi G, Cembran A, Bernardi F (2004). J Am Chem Soc 126:3234–3243
47. Cimiraglia R, Hofmann HJ (1994). Chem Phys Lett 217:430–435
48. Hernández-García L, Sandoval-Lira J, Rosete-Luna S, Niño-Medina G, Sanchez M (2018). Struct Chem 29:1265–1272